

Recent Progress in the Development of Organic Chemosensors for Formaldehyde Detection

Ahmed Abu-Rayyan, Imtiaz Ahmad,* Nawal H. Bahtiti, Tahir Muhmood,* Samir Bondock, Mohammed Abobashrh, Habiba Faheem, Nimra Tehreem, Aliya Yasmeen, Shiza Waseem, Tayabba Arif, Amal H. Al-Bagawi, and Moaz M. Abdou*

Cite This: *ACS Omega* 2023, 8, 14859–14872

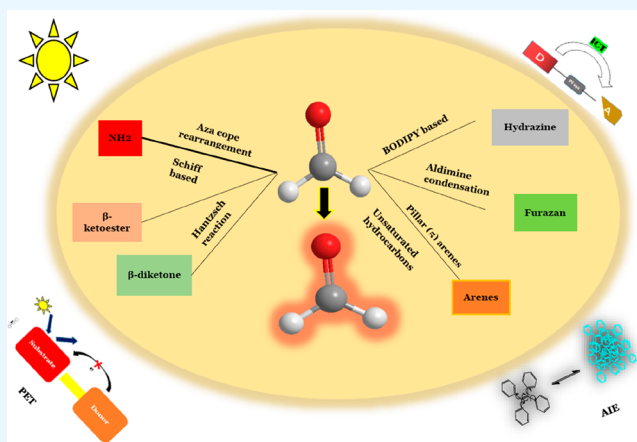
Read Online

ACCESS |

Metrics & More

Article Recommendations

ABSTRACT: Formaldehyde has become a prominent topic of interest because of its simple molecular structure, release from various compounds in the near vicinity of humans, and associated hazards. Thus, several researchers designed sophisticated instrumentations for formaldehyde detection that exhibit real-time sensing properties and are cost-effective and portable with high detection limits. On these grounds, this review is centered on an analysis of optical chemosensors for formaldehyde that specifically fall under the broad spectrum of organic probes. In this case, this review discusses different organic functionalities, including amines, imines, aromatic pillar arenes, β -ketoesters, and β -diketones, taking part in various reaction mechanisms ranging from aza-Cope rearrangement and Schiff base and Hantzsch reactions to aldimine condensation. In addition, this review distinguishes reaction mechanisms according to photophysical phenomena, that is, aggregation-induced emission, photoinduced electron transfer, and intramolecular charge transfer. Furthermore, it addresses the instrumentation involved in gas-based and liquid formaldehyde detection. Finally, it discusses the gaps in existing technologies followed by a succinct set of recommendations for future research.



1. INTRODUCTION

Formaldehyde (FA) is a highly reactive volatile organic compound with varying concentrations not only in the environment but also in the human body. It can react with various compounds such as hydroxyl ($-\text{OH}$), sulfhydryl ($-\text{SH}$), and carboxyl ($-\text{C}=\text{O}$) groups and compounds such as water, ethanol, and amino acids.¹ This is one of the reasons for the existence of FA in various forms, ranging from monomeric FA to diol, polymers, and trimers found as methanediol, paraformaldehyde, and trioxane. In addition, it is active in both its gaseous and liquid forms. The half-life of this compound is only 1 h but still is found in different environments.² As per the data provided by the Agency for Toxic Substances and Disease Registry, the level of FA in indoor air is between 0.02 and 4 ppm, whereas that in outdoor air ranges from 0.0002 to 0.006 ppm.³ Consequently, FA is a potential carcinogen and is involved in several chronic diseases, including heart diseases, cancers, diabetes, and neurodegenerative diseases. In this case, Wan et al. mentioned that FA is emitted from highly common sources like plywood, cosmetics, textiles, fiberboard, and even cigarettes.⁴ In addition, FA is endogenously produced from amino acids such as serine,

choline, and methionine.⁵ Such interesting chemistry of FA, along with high human exposure, is evident in the significant amount of empirical literature that aims at efficient FA detection in both liquid and gaseous forms under various *in vivo* and *ex vivo* experimental conditions.

On the basis of such a significant need for FA detection, several sensors have been manufactured (e.g., electrochemical, optical, photochemical, and FA gas sensors) operating on several different techniques, such as fluorometry, conductometry, colorimetry, amperometry, piezoresistivity, and spectrophotometry. On these grounds, Chung et al. analyzed FA gas sensors and concluded that these sensors are highly efficient, have small sizes, show low power consumption, and provide real-time responses.⁶ However, they found that some gas-based sensors have low detection limits. In contrast, Kukkar et al.

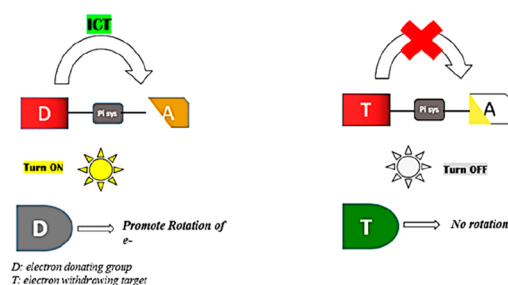
Received: December 4, 2022

Accepted: March 31, 2023

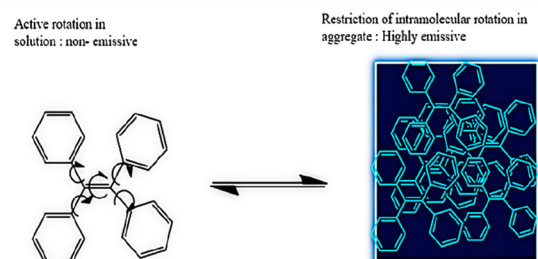
Published: April 17, 2023



1. Intramolecular charge transfer



2. Aggregation induced emission



3. Photo induced electron transfer



Figure 1. Photophysical phenomena operative in FA detection.

reviewed electrochemical sensors by specifically focusing on nanoscale sensors. Electrochemical sensors have low costs, and their structures are not complex. However, these nanoscale sensors are found to be less specific and less stable and cannot be produced in substantial amounts. In addition, they are exposed to interferences due to the reaction of electrolytes with FA.⁷

In another study, Xu et al. scrutinized the significance of optical chemosensors and inferred that fluorescence-based sensors have an exceptionally noninvasive nature and high sensitivity and can easily detect minute changes in wavelength, making them more suitable for cellular detection.⁸ Also, optical chemosensors are cost-effective and easier to handle than chromatographic and spectroscopic instrumentations, which are larger, more expensive, and more difficult to operate.⁹ Pan et al. specifically worked on amine-based probes by focusing on their polymeric versions.¹⁰ Meanwhile, Lin et al. proposed a unique dimension and worked on pillar arenes for FA detection.¹¹ Similarly, Bi et al. investigated the role of naphthalamide-based probes in detecting FA.¹² However, despite the significant amount of literature on FA detection, previous studies mostly focused on either one specific reaction mechanism or one specific functionality. In addition, an extensive amount of research data proffers a need for a more integrated approach. Continuing our research on organic compounds and their applications,^{13–17} this review aims to adopt a novel approach to categorizing reactions based on reaction mechanisms and organic functionalities taking part in FA detection.

2. PHOTOPHYSICAL FA DETECTION MECHANISMS

Optical chemosensors operate on different photophysical phenomena in FA detection. According to Misra and Bhattacharyya, intramolecular charge transfer (ICT) is the flow of electrons from a donor species to an acceptor species.¹⁸ In this case, the electron-donating groups promote the rotation of electrons, which is the basic driving force behind charge transfer. Consequently, the species fluoresce, showing a “turn-on” mechanism; meanwhile, electron-withdrawing groups cannot bring about such rotation of electrons, and hence no

charge transfer occurs. In organic molecules, ICT occurs through a p-electron bridge, and the process is known as through-bond charge transfer. If there is no p-electron bridge, the charge transfer mechanism is called through-space charge transfer.¹⁸

On these grounds, Natali et al. identified photoinduced electron transfer (PET) in organic molecules and mentioned that PET involves the electron transfer from an electron-rich donor to an electron-deficient acceptor. Upon light excitation, a hole creates in the donor, and the acceptor becomes an electron-rich radical.¹⁹ For this electron transfer, Ma et al. defined mechanisms according to which photoexcitation in the donor excites the electrons from H from the highest occupied molecular orbital (HOMO) to the lowest unoccupied molecular orbital (LUMO), whereby this LUMO then transfers the electron to the LUMO of the acceptor (d-pet).²⁰ Alternatively, the HOMO of the acceptor can also donate electrons to the unfilled HOMO of the donor (occurring as a-pet). Moreover, some organic fluorophores show contrasting behaviors from the solution to their aggregated state. Upon aggregation, a fluorescent enhancement evidently follows the mechanism of aggregation-induced emission (AIE). There is a nonemissive behavior in the solution state due to active rotation; however, upon aggregation, intramolecular rotation is restricted, thus turning on the fluorescence.²¹ As per empirical evidence, this review discusses the application of these photophysical phenomena in optical FA detection (Figure 1).

3. GAS- AND LIQUID-BASED ANALYZERS FOR FA DETECTION

A gas-based colorimetric analyzer for FA consists of an automotive device that consists of trapping units, a detector, and a flow meter. The adsorbent used is silica gel, which is incorporated into a solution and dried. A system for sensitive FA detection is maintained on the basis of color change after the reaction of FA with the adsorbent. An optical system consisting of a light-emitting diode (LED) is used for FA detection. The detection limit of the analyzer is 80 ppb for 30 min.²²

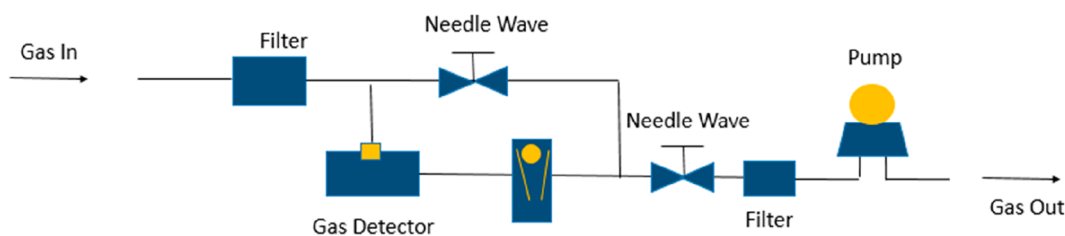


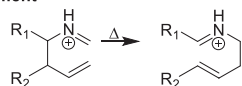
Figure 2. Flow injection analysis method for FA detection.

Another method of FA detection is based on the flow injection analysis scheme (Figure 2). A reagent solution is added to the system to achieve a suitable baseline, followed by the addition of FA through an injection valve. The reaction coil then takes up the mixture of FA and reagent. The optical system measures the absorbance change using an LED, and the monitor records the resulting peaks.²³ The first method is based on the detection of gaseous FA based on color change due to interactions with the adsorbent-doped surface, whereas the second method involves the uptake of FA into the aqueous solution and the measurement of its absorbance change.

4. ORGANIC CHEMOSENSORS

4.1. NH₂-Based Probes. Several researchers have contributed to the identification of NH₂-based probes for FA

Aza-Cope rearrangement



Proposed mechanism



Figure 3. Aza-Cope rearrangement reactions.

detection. This is highly evident, for instance, through the research of Manna et al., which showed that many NH₂-based probes follow aza-Cope rearrangement reactions. Aza-Cope rearrangement is basically a sigmatropic-rearrangement-centered reaction where a [3,3] bond shifting occurs.²⁴ This occurs in the primary compound of 1,5-hexadiene substituted with nitrogen. The mechanism proceeds through an intermediate chairlike structure. The rearrangement shifts single and double bonds between two allylic parts.²⁵ In this case, sigmatropic rearrangements are involved in pericyclic reactions, where the σ bond in the adjacency of pi systems is transferred and the overall pi system reestablishes itself (Figure

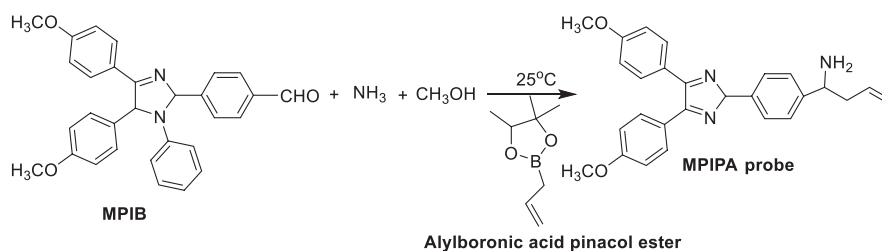


Figure 4. Synthesis of the MPIPA probe.

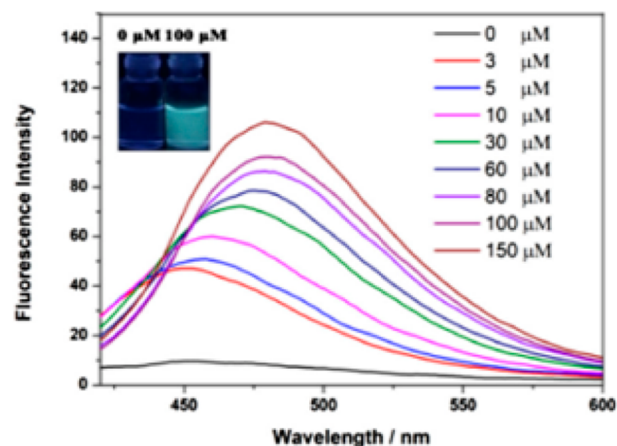


Figure 5. FA detection at different MPIPA concentrations. Reprinted with permission from ref 27. Copyright 2018 Elsevier.

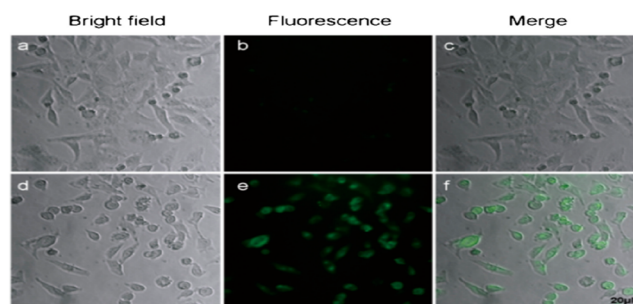


Figure 6. Fluorescent imaging of cancer cells. Reprinted with permission from ref 27. Copyright 2018 Elsevier.

3). The total number of sigma and pi bonds is preserved in the end. Moreover, they are intramolecular in their attribution.²⁶

According to the above mechanism, Gao et al.²⁷ synthesized the 1-(4-(4,5-bis(4-methoxy-phenyl)-1-phenyl-1H-imidazol-2-yl)phenyl)but-3-en-1-amine (MPIPA) probe for the cellular detection of FA. The MPIPA probe reacts with FA molecules to form the MPIPA compound. FA molecules, upon reacting with MPIPA, generate iminium ions, which facilitate 2-azo-Cope

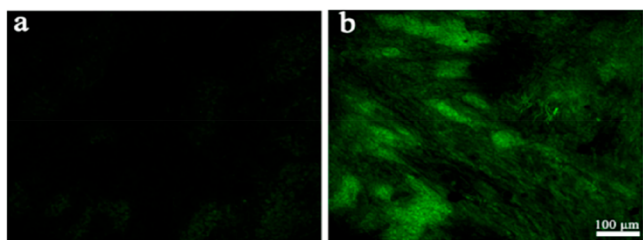


Figure 7. (a,b) Fluorescence showed by MPIPA in the presence of FA. Reprinted with permission from ref 27. Copyright 2018 Elsevier.

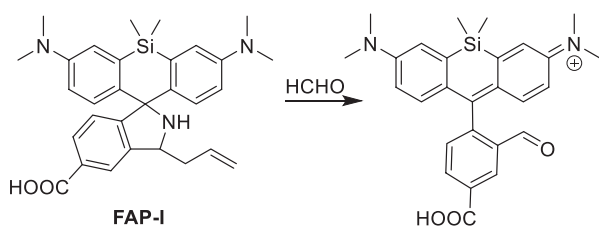


Figure 8. FAP-I-aided detection of FA.

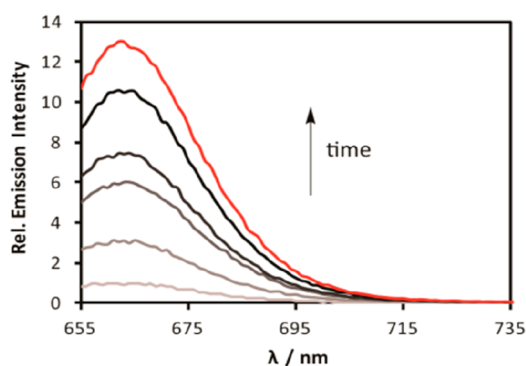


Figure 9. FA detection at different concentrations. Reprinted with permission from ref 31. Copyright 2015 American Chemical Society.

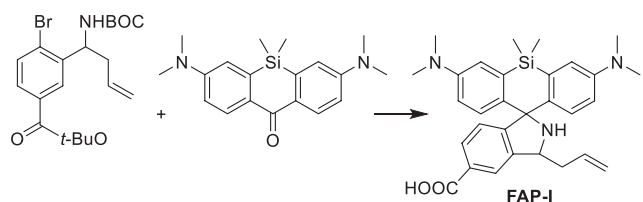


Figure 10. Synthesis of the FAP-I probe.

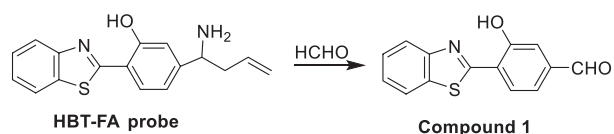


Figure 11. HBT-FA detection mechanism of FA.

rearrangement (Figure 4). In this process, homoallylamino changes into an aldehyde group in MPIB that aids in the fluorescence detection of MPIB. The MPIPA probe detects FA through AIE and twisted ICT. In the compound MPIB, ICT occurs from the electron-donating methoxy group to the electron-withdrawing aldehyde. In this case, the HOMO orbital is present on the electron donor methoxy-substituted phenyl ring and imidazole groups, whereas the LUMO and

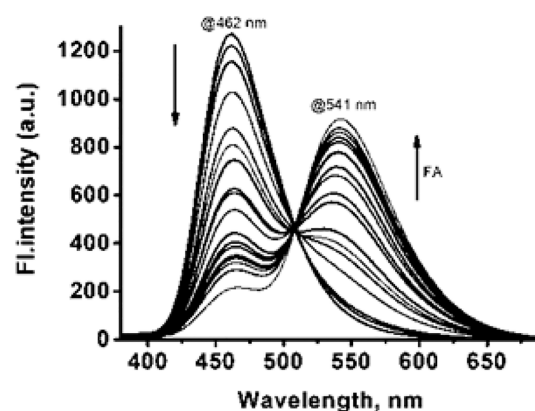


Figure 12. FA detection with increasing concentration. Reprinted with permission from ref 33. Copyright 2017 Elsevier.

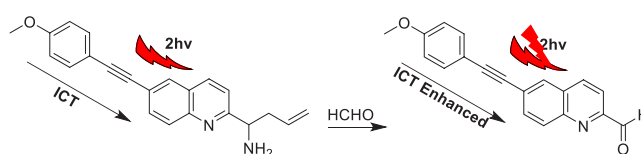


Figure 13. MQAP probe reaction with FA.

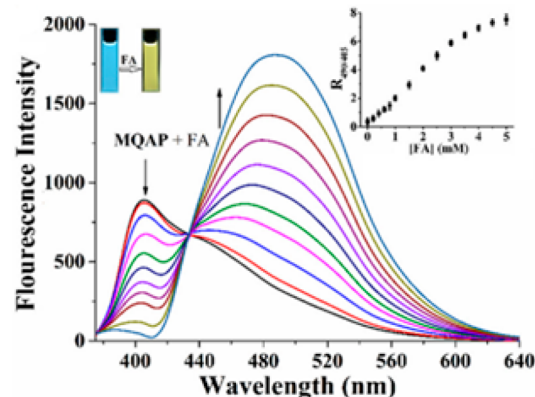


Figure 14. Fluorescence spectra of the MQAP probe at different FA concentrations. Reprinted with permission from ref 35. Copyright 2018 Elsevier.

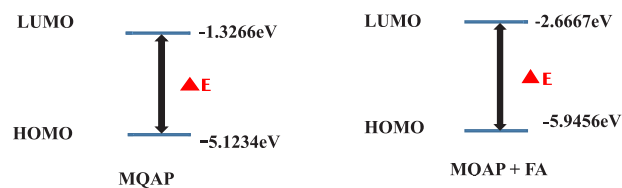


Figure 15. Density functional theory calculations of MQAP and MQAP + FA.

LUMO+1 orbitals are located on the electron-withdrawing aldehyde group (i.e., 4-formylphenyl group). As a result of such a charge distribution, ICT occurs on the MPIB, which is responsible for its fluorescence. The reaction takes place in a dimethyl sulfoxide/water mixture. Consequently, the emission of MPIB is highly dependent on the solvent concentration; when the water fraction is increased to about 80% to 99%, the MPIB probe shows AIE because of its poor solubility in high

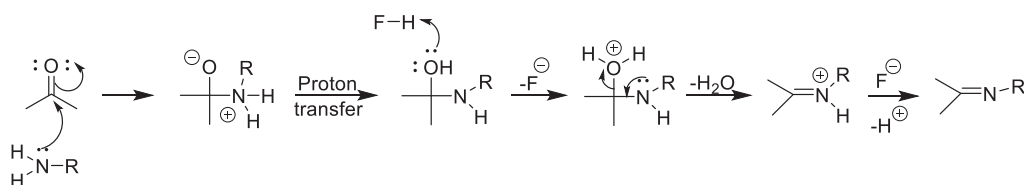


Figure 16. Schiff base mechanism.

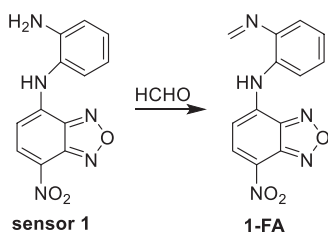


Figure 17. Mechanism of detection of sensor 1 toward FA.

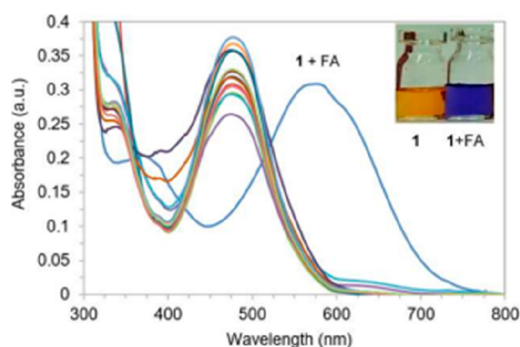


Figure 18. Absorption spectrum upon FA addition. Reprinted with permission from ref 39. Copyright 2020 Elsevier.

water content. Thus, the fluorescence maximum decreases from 530 to 495 nm.²⁷

When the MPIPA probe was in the free state, it exhibited weak emission at 380 nm. However, when FA was added in the concentration of 3 μM to 150 μM , the fluorescence intensity showed a marked increase from 450 to 485 nm as a result of the redshift. Thus, for the MPIPA probe, the fluorescence intensity increases with the increase in the concentration of formaldehyde (Figure 5).²⁷

As the study specifically focused on the cellular detection of FA, the treatment of HeLa cells with 10 μM of the MPIPA probe in the absence of FA showed no fluorescence (Figure 6). Nonetheless, the above-mentioned treatment in the presence of 50 μM of FA showed fluorescence in both the fluorescence and merged fields (Figure 6). A detection limit of 123 nM was achieved.²⁷

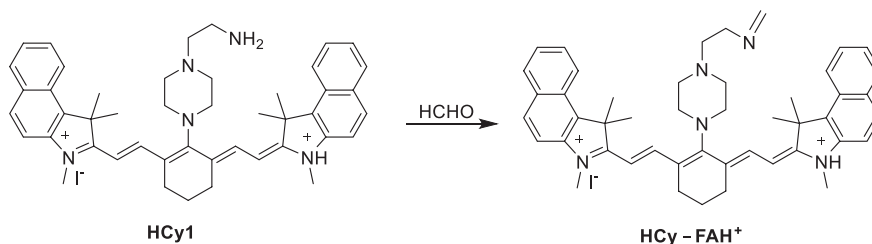


Figure 19. FA detection mechanism of HCy1.

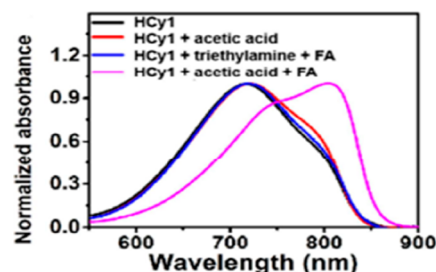


Figure 20. Absorption spectrum of HCy1 under different situations. Reprinted with permission from ref 41. Copyright 2019 Elsevier.

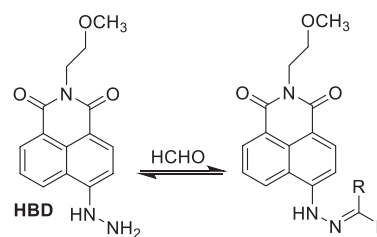


Figure 21. FA sensing mechanism of HBD.

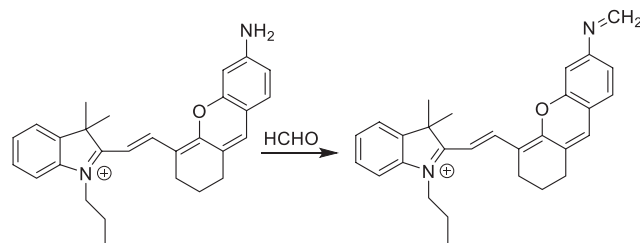


Figure 22. FA detection mechanism of the probe-NH₂.

Similarly, the MPIPA probe efficiently detected FA in breast cancer tissues. In the absence of FA, MPIPA showed no fluorescence (Figure 7a). In contrast, green fluorescence appeared in the presence of FA (Figure 7b).

Upon analyzing the efficiency of probe, it becomes highly evident that the MPIPA probe used in this study has an ultralow detection limit of 123 nM for specific cellular (Hela cells) detection of FA. In this context, Xu et al.²⁸ focused

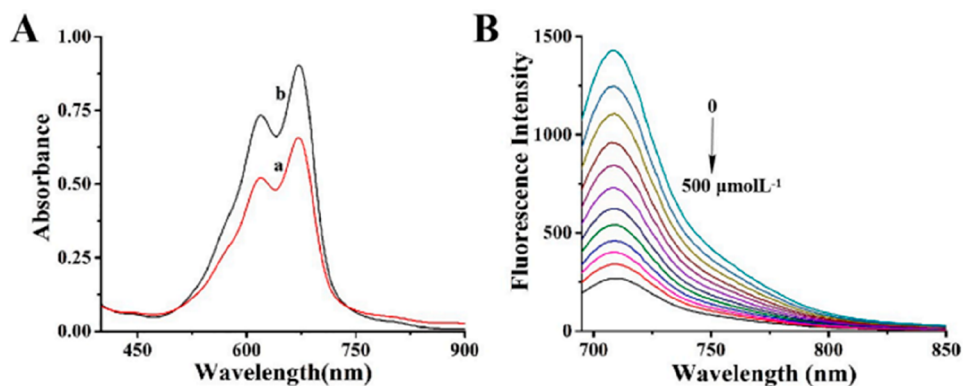


Figure 23. (A) Absorption spectra of probe-NH₂ before (a) and after (b) reaction with FA. (B) Fluorescence spectra with FA. Reprinted with permission from ref 43. Copyright 2022 Elsevier.

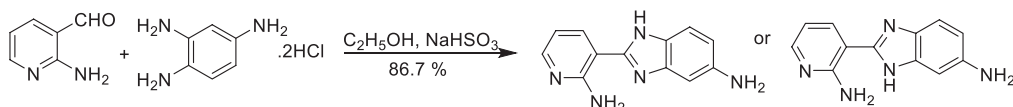


Figure 24. Synthesis of the 2-amidyl-3-(3-amidyl-1H-benzo[d]imidazolyl)-pyridine probe.

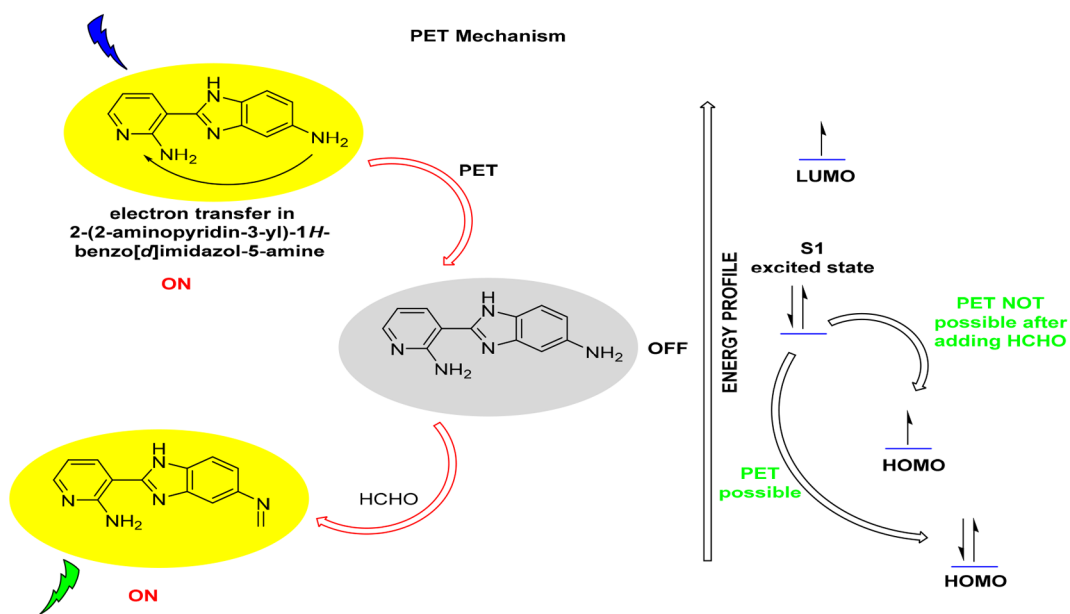


Figure 25. PET mechanism operative in the 2-amidyl-3-(3-amidyl-1H-benzo[d]imidazolyl)-pyridine probe. Reprinted with permission from ref 44. Copyright 2014 Elsevier.

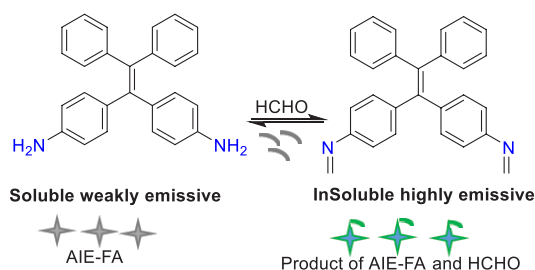


Figure 26. Illustration of the fluorescence turn-on mechanism for FA detection and imaging.

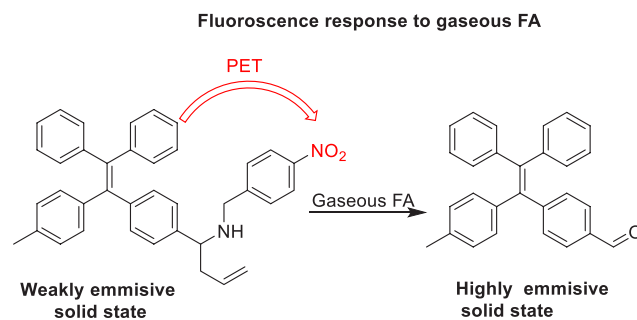


Figure 27. Response mechanism to FA.

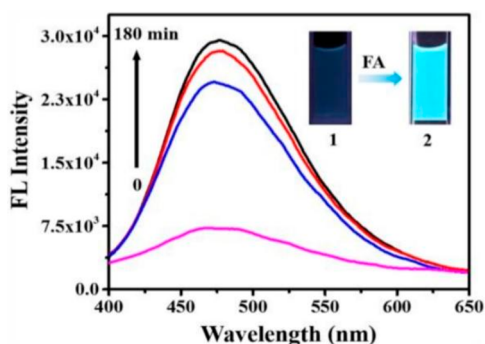


Figure 28. Time-dependent fluorescence spectra of TPE-FA. Photographs of TPE-FA in the absence (1) or presence (2) of FA for about 180 min under a UV lamp. Reprinted with permission from ref 48. Copyright 2018 American Chemical Society.

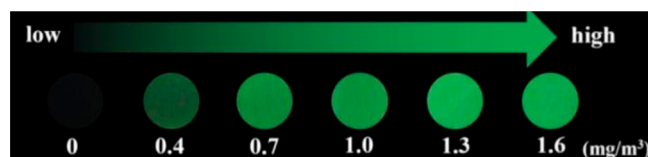


Figure 29. Photographs of FA test plates incubated with various concentrations of gaseous FA for 60 min under a UV lamp. Reprinted with permission from ref 48. Copyright 2018 American Chemical Society.

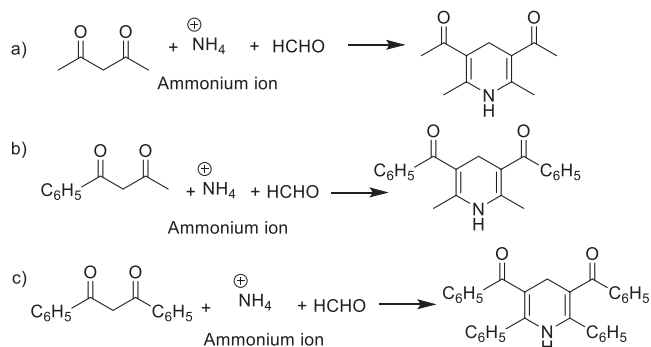


Figure 30. (a–c) Reaction of FA with three diketones.

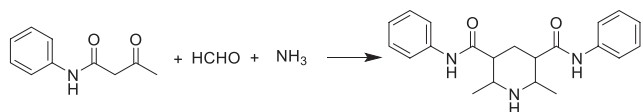


Figure 31. Reaction of acetacetanilide with FA.

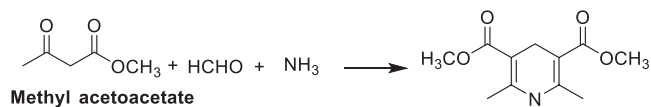


Figure 32. Reaction of methyl acetoacetate with FA.

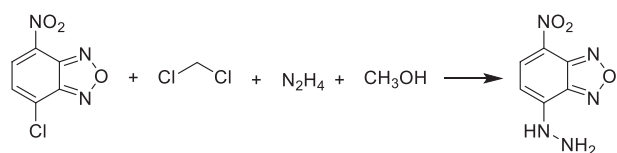


Figure 33. Synthesis of the NBD-based FAP probe.

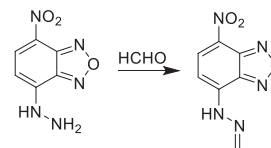


Figure 34. Detection mechanism of the FAP probe.

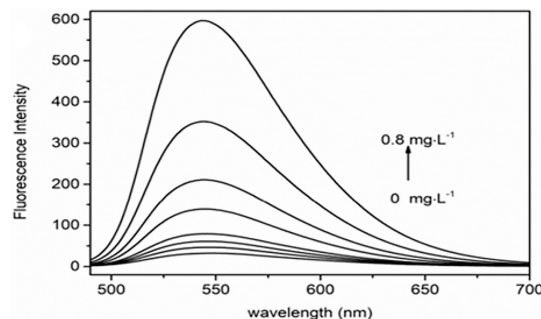


Figure 35. Relationship with the FA concentrations. Reprinted with permission from ref 54. Copyright 2020 Elsevier.

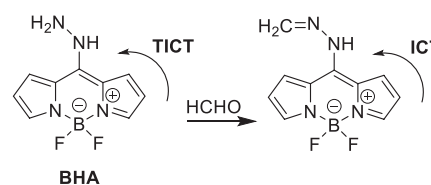


Figure 36. FA detection by BHA.

specifically on naphthalene-based probes and conducted a similar study on HeLa cells but achieved the detection limit of 570 nM that also marks the high sensitivity of the MPIPA probe in comparison to the naphthalene-based probe. Nonetheless, for intracellular detection, probe design is significantly important because it determines the selectivity of probe. In this case, the MPIPA probe exhibited 4–6 times better response to FA than other analytes, but modern grafting techniques such as used by Liu et al.²⁹ in the form of an efficient “multi-lock system -key-and-lock”-based NBC probe bring high selectivity and high cellular retention time to the probes, which is a design limitation of the MPIPA probe. Similarly, the MPIPA probe requires a 2 h incubation period, which is another limitation of the probe in comparison to ultrafast fluorescent probes.³⁰ Brewer and Chang synthesized the FAP-I probe for the detection of reactive carbonyl species (FA) in living systems (Figure 8). Based on aza-cope rearrangement, in the presence of formaldehyde, homoallylic amine that is weakly fluorescent due to a closed ring is transformed into an aldehyde group with an open ring and more fluorescence.³¹ This gives a turn-on fluorescence response. FAP-I is weakly fluorescent due to spirocyclization of homoallylic amine but shows an 8-fold increase in its fluorescence activity upon addition of formaldehyde as it inhibits spirocyclization (Figure 8).³¹

As the FA concentration was increased from 10 to 100 μM , the fluorescence intensity increased, with an excitation wavelength of 645 nm and an emission wavelength of 662 nm. The increase in absorbance was also measured (Figure 9).

The FAP probe showed good solubility ($\log D_{\text{oct/wat}} = 0.53 \pm 0.01$) in aqueous solutions with 100 μM FA concentration. The detection limit of FAP-I was found to be 5 μM for FA

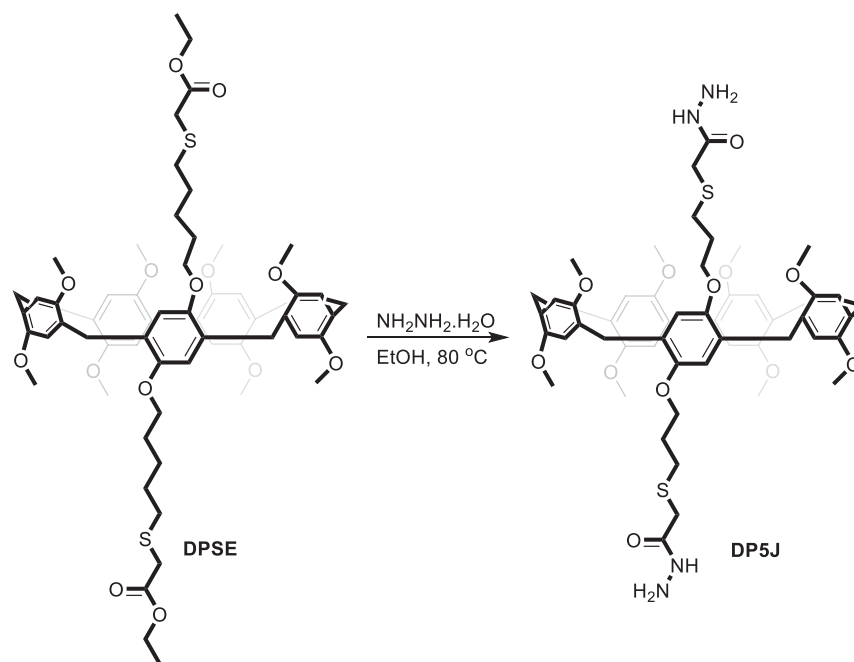


Figure 37. Synthesis of DP5J.

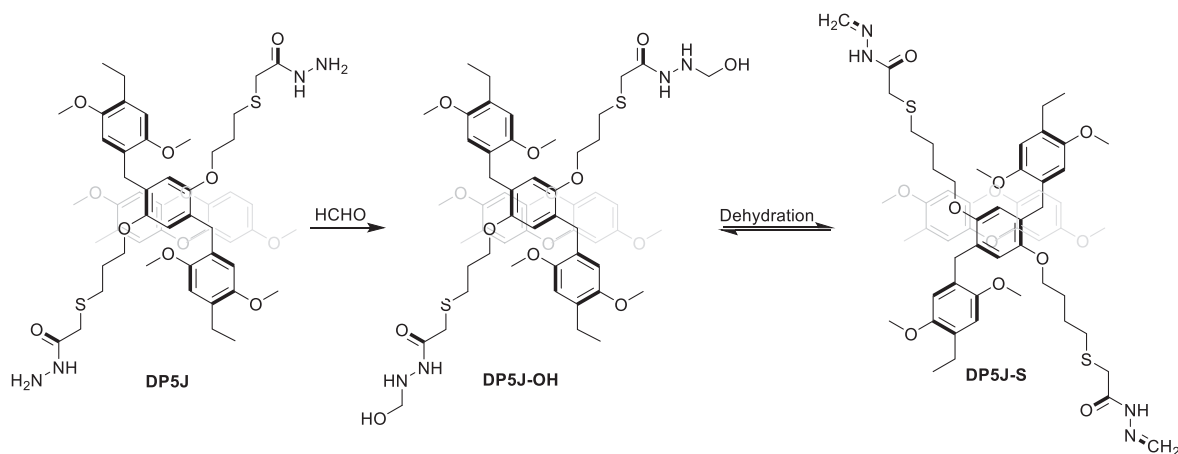


Figure 38. FA detection mechanism of the DP5J probe.

detection. At the laser power of 6%, FAP-I displayed enhanced fluorescence up to 100 scans, but the FAP-I probe was shown to display photobleaching at a laser power of 50%. Although the first-generation FAP-I showed selective detection of FA in endogenous cells, it functions by directly incorporating its moiety into the fluorophore scaffold due to the fluorescence being dependent on spirocyclization.³² Synthesis of FAP-I takes place in a series of steps through boronate-mediated aminoallylation (Figure 10).³¹

Zhou et al. demonstrated how the reaction of the ratiometric fluorescent HBT-FA probe with FA gives compound **1** based on the ICT mechanism (Figure 11).³³ The HOMO and LUMO of the HBT-FA probe and compound **1** operated on the electron transfer mechanism as the energy gaps between the HOMO and LUMO of these respective compounds were 3.365 and 3.065 eV. The π electrons on the HOMO and LUMO of HBT-FA were practically dispersed over the complete 2-(2-hydroxyphenyl)benzothiazole skeleton. The π electrons of compound **1**, in comparison, showed variations in the π electrons of the LUMO being dispersed over the entire

molecular scaffold and the π electrons of HOMO being essentially dispersed over 2-(2-hydroxyphenyl)benzothiazole.³³

Increasing the concentration of FA increased the fluorescence intensity. The maximum absorption peak (333 nm) of HBT-FA in the absence of FA changed to 350 nm in the presence of FA (Figure 12).³³ The HBT-FA probe showed a strong emission band at 462 nm after excitation at 350 nm. The emission intensity increased further to 541 nm, and the emission peak of 462 nm decreased after increasing the FA concentration (0–30 mM) (Figure 12). The increase in the emission intensity at 541 nm was attributed to the strong push–pull electronic process because of the formation of compound **1**. The fluorescence intensity ratio (F541/F462) increased in the presence of FA to 4.30 but was 0.11 in the absence of FA. The emission rate increased by 39-fold by increasing the concentration of FA.

The detection limit of the HBT-FA probe was found to be $4.1 \times 10^{-4} \mu\text{M}$ at a pH of 7.4. Meanwhile, the fluorescence intensity was found to be highly time-dependent and showed a marked change in a period of 7 h. The probe, however, showed

selectivity for FA over the other tested reagents. When calf serum samples were detected, HBT-FA showed lower fluorescence intensities with increasing calf serum concentrations. Meanwhile, the synthesized BT-I probe was highly selective and took 3 min to show its fluorescence intensity.³⁴ In another study, a two-photon fluorescent probe, MQAP, based on the aza-Cope mechanism was synthesized by Yang et al. for FA detection. The MQAP probe originally showed a short emission wavelength of 405 nm.³⁵

The probe core structure contains 1-ethynyl-4-methoxybenzene with a homoallylamine group bonded with quinoline. The homoallylamino group serves as a reaction site for FA detection. When FA is added, the homoallylamino group reacts with FA; an imine intermediate is then formed, which is further converted into aldehyde through 2-aza-Cope rearrangement followed by hydrolysis. Figure 13 shows the two-photon detection of FA using the MQAP probe.³⁵

Upon the addition of FA, a redshift in the emission wavelength of MQAP was observed. The redshift was caused by enhancement in the ICT process from the electron donor methoxy phenyl alkenyl group to the electron acceptor aldehyde group upon two-photon light absorption. The FA detection limit of the MQAP probe was found to be 4.054 μM .³⁵ Figure 14 shows the increase in fluorescence intensity as the FA concentration is increased.

Through density functional theory calculations, the energy gaps between the HOMO and LUMO of MQAP and MQAP+FA were found to be 3.7968 and 3.2789 eV, respectively (Figure 15). The relatively lower energy gap between the HOMO and LUMO of MQAP+FA resulted in a redshift with an emission wavelength of 490 nm. This also suggested that the incorporation of the homoallylamino group into the core fluorophore structure would be effective for FA sensing.³⁶

FA was detected in MCF-7 cells using the MQAP probe. The advantages of this probe include its low cytotoxicity, insensitivity to pH change, and deep tissue penetration up to 150 μm . However, its low sensitivity (with a detection limit of 4.054 μM) and long response time limit its use for FA detection in MCF cells. Recently, a new aza-Cope rearrangement based on an AFP ratiometric probe was synthesized, which displayed a response time of less than 20 min and showed high sensitivity (with a detection limit of 66 nM).³⁷

Under the broader categories of NH_2 -based probes, some probes also follow a Schiff base mechanism. In this case, primary amines condense with carbonyl groups to generate a Schiff base in a nucleophilic addition reaction. Typically, the nitrogen of amine groups acts as a nucleophile and attacks carbonyl carbon. In the next step, the deprotonation of nitrogen results in the formation of the imine product through the displacement of the water molecule (Figure 16).³⁸

According to the above mechanism, Wechakorn et al.³⁹ worked on an N^1 -(7-nitrobenzo[*c*][1,2,5]oxadiazol-4-yl) benzene-1,2-diamine sensor for FA detection. The absorption spectrum showed a peak at 475 nm. Upon the addition of FA, the color of the solution transitioned from yellow to deep purple. This new solution then exhibited a peak at 582 nm, whereas the intensity of the peak at 475 nm was reduced (Figures 17 and 18).³⁹ The former probe has a lower LOD with 30 μM (0.03 M) than the CHA probe (0.20 M).⁴⁰

Wei et al. took HCY as a chromophore, and a pH-sensitive piperazine moiety was inserted into it along with an FA-sensitive primary amine moiety to produce FAHCY-FAH⁺ (Figure 19).⁴¹ Upon reaction with FA, HCY1 showed a color

change from blue to green in a weakly acidic environment (pH 3–6); in contrast, it stayed blue in basic or neutral conditions.⁴¹ During the reaction of HCY1 with FA and acetic acid, the color changed to green with shifting toward 800 nm, and the fluorescence intensity was reduced (Figure 20). The absorption maxima of HCY1 remained unaltered only under the FA or acetic acid conditions. The researchers observed that under acidic environments protonation occurred at two nitrogen atoms of piperazine, disturbing the ICT. This then led to a redshift of the absorption maxima and resulted in colorimetric changes.⁴¹

Lu et al. found that the HBD probe, upon its addition to aldehyde, resulted in the formation of an imine product (Figure 21).⁴² When the HBD probe was immersed in the FA solution, the fluorescence spectra showed different emission intensities at 550 nm. The fluorescence intensities slowly increased upon the increase in infiltration volume of 15 μL to approximately 30 μL . The maximum emission wavelength was observed at 550 nm.⁴²

The FA detection mechanism found by Ding et al. (probe- NH_2) is a Schiff base reaction where an amino group over the course of FA addition gets converted into imines. Therein, $\text{C}=\text{N}$ can further affect the PET process (Figure 22).⁴³

Ding et al. found a maximum absorption peak in the region of 670 nm, where a shoulder peak at 620 nm was also observed for a probe solution with FA, as shown in Figure 23(A). In addition, they studied the fluorescence intensity depicted in Figure 23(B) by varying the concentrations of the FA solution; 500 $\mu\text{mol L}^{-1}$ was added, which intensified the absorption peak. However, the FA concentration had an inverse effect, which decreased the fluorescence intensity, while the concentration continued to increase.⁴³ The advantage of the probe- NH_2 is that it has greater use in biological systems, as in mice. This probe is also very highly efficient as it has a recovery range of 99.0%–110%. Moreover, it is efficiently used in FA detection in food. Further, it is highly selective and sensitive as its detection limit is 1.87 μM , which is higher than those of the HBD probes.⁴³

Zhou et al. used a dual model fluorescent probe 2-amidyl-3-(3-amidyl-1*H*-benzo[*d*]imidazolyl)-pyridine for the detection of FA (Figure 24).⁴⁴ The compound was described as a dual emissive probe, as upon excitation at 365 nm, the compound showed weak fluorescence emission at both 409 and 515 nm, respectively. The working mechanism of this probe depends on the photoinduced electron transfer (PET) mechanism, where when the probe was in the free state the electron transfer occurred from the aniline group to the pyridine group that resulted from the quenching of the probe. However, upon reaction with FA, an imine group forms on the probe. Such a process inhibits the PET mechanism due to the electron-deficient nature of the imine group in comparison to the aniline group.⁴⁴

The formation of the imine group actually disturbed the energy distribution of the HOMO of the above probe. Before the imine formation, the HOMO of the probe was at -5.014 eV. After the imine formation, the HOMO decreased in energy to -5.382 eV, thereby preventing PET. The free probe showed emission at 515 nm; however, the introduction of FA eliminated the formation of this peak, and a redshift appeared from 409 to 415 nm (Figure 25). In this case, the detection limit of the probe reached as low as 6 μM .⁴⁴

As per the above analysis, the 2-amidyl-3-(3-amidyl-1*H*-benzo[*d*]imidazolyl)-pyridine probe is a dual emissive probe

with high sensitivity. Such added efficiency was also justified by the research of Kukhta and Bryce, according to whom pure organic dual emissive molecules are highly sensitive because they can distinguish between false positive signals and required signals.⁴⁵ However, the probe had a detection limit of 6000 nM, which is less sensitive compared with those of new and modified R-C=N-functionality-based probes. For instance, Ji et al. developed R-C=N-functionality-based D-A type [2.2]paracyclophanyl-4H-pyran-4-one fluorescent probes for the detection of FA and other acidic gases and achieved a detection limit in the ppm scale that ranged from 1.39 to 8.75 ppm. Moreover, the probes detected FA within 5–7 s, which is a much better response time than that of the 2-amidyl-3-(3-amidyl-1H-benzo[d]imidazolyl)-pyridine probe at 48 s.⁴⁶

A fluorescent probe for FA detection based on AIE was designed by Chen et al. (Figure 26) and was featured for its fast sensitivity and selectivity.⁴⁷ This FA-responsive AIE probe was synthesized through the introduction of two FA-reactive amine groups in tetraphenylethene (Figure 26). These two amine groups not only function as reactive moieties for FA but also increase its solubility. AIE-FA is nonfluorescent in its dissolved state. However, upon its condensation with FA, the amine groups are converted into Schiff bases. This results in low solubility and hence the formation of aggregates. This consequently turns on the fluorescent signal due to typical AIE phenomena due to the restriction of the intramolecular rotation-induced energy dissipation pathway.

Using the aqueous solubility differences between the amine-functionalized “AIEgens”, as well as the Schiff-base-modified AIE “molecules” after reaction with FA, a highly sensitive and rapid assay for FA was readily achieved.⁴⁷ The probe was demonstrated to possess rapid response, great selectivity, and high sensitivity toward FA *in vitro*. Moreover, AIE-FA exhibited a fast response toward FA in real time in living cells. Thus, AIE-FA has great potential in sensing FA concentrations in living systems under various physiological conditions. However, the AIE-FA probe requires an incubation period of about 1.5 h, which is its limiting factor compared with other ultrafast probes.

4.2. Unsaturated Hydrocarbons. In another study, Zhao et al. synthesized an AIE-based fluorescent probe for the detection of gaseous FA (TPE-FA).⁴⁸ Ph-NO₂ was incorporated into TPE-FA to quench the fluorescence of TPE to get a fluorescence turn-on response. Initially, TPE-FA had a weak fluorescence because of PET between the electron donor (TPE-H-NH₂) and the electron acceptor (Ph-NO₂). However, upon condensation with FA, a weakly emissive TPE-FA was converted into a highly emissive compound, which thus showed fluorescence (Figure 27). Thus, TPE-FA can detect FA through the fluorescence turn-on response. An FA test plate was easily fabricated by directly loading TPE-FA in high-performance thin-layer chromatography. The test plate can achieve high sensitivity and selectivity for the detection of gaseous FA.

TPE-FA was successfully developed for the detection of FA and exhibited a fluorescence turn-on response to FA. As an AIE-based solid sensor for gaseous FA, the FA test plate enables convenient use and transport as compared with solution-based sensors. As shown in Figure 28, in the absence of FA, TPE-FA showed no fluorescence. Upon the addition of FA at a wavelength of 480 nm, the FL intensity increased up to 4-fold in 180 min, thus indicating the fluorescence turn-on property of TPE-FA for the detection of FA (Figure 28).⁴⁸

Figure 29 shows photographs of FA test plates incubated with gaseous FA under a UV lamp of wavelength 365 nm for about 60 min.⁴⁸ The fluorescence changes of the test plates before and after their reaction with gaseous FA can be observed by the naked eye under a UV lamp (Figure 28). Therefore, given such high sensitivity, the TPE-FA-loaded test plates acted as easy and mobile sensors for the detection of gaseous FA by the naked eye.⁴⁸

TPE-FA exhibits a “turn-on” fluorescence response to FA through 2-aza-Cope sigmatropic rearrangement. By a simple preparation process, the FA test plate was obtained. The test plate was found to achieve sensitive, selective, and facile detection of gaseous FA through fluorescence “turn-on” detection. The detection limit is 0.036 mg/m³, which is lower than the air quality guideline value of gaseous FA (0.1 mg/m³). Moreover, the detection results are obvious and easy to be observed with the naked eye. As an AIE-based solid sensor for gaseous FA, FA test plates enable safer and more convenient use and transport compared to solution-based sensors (Figure 29).⁴⁸

4.3. β -Ketoester and β -Diketone. Formaldehyde-based sensors based on Hantzsch reaction for detecting formaldehyde are made with the reaction of beta diketone or beta ketoester and ammonium ions acting as a nitrogen donor along with formaldehyde. The formaldehyde-sensing elements for detecting trace formaldehyde are synthesized on a porous glass surface and do not require the need to separate the intermediate material.

After exposure to FA, initially colorless sensor elements turn yellow. The yellow color is an indication of the formation of a colored pyridine called lutidine. In this regard, Maruo et al. reported the reaction mechanism of three beta diketones (acetylacetone, 1-phenyl-1,3-butanedione, and 1,3-diphenyl-1,3-propanedione) (Figure 30a–c).⁴⁹

Change in absorbance is recorded by exposing beta diketone in ammonium ions and an acetic acid environment to different concentrations of formaldehyde. In the absence of FA, the conjugated electrons of acetylacetone show an absorption wavelength below 340 nm. In the presence of FA, as the formaldehyde concentration increases, the absorbance peak increases and appears at 407 nm. There is a clear gap between the absorption peak of acetylacetone before the addition of formaldehyde and after the addition of formaldehyde. When the sample, i.e., acetylacetone along with diketone and an ammonium ion, is placed in pure water inside the tedler bag there is no absorbance peak shown at 407 nm. So, the absorbance peak at 407 nm is the result of the addition of formaldehyde to the above reaction mixture. For 1-phenyl-1,3-butanedione, in the absence of FA, the conjugated electrons of 1-phenyl-1,3-butanedione show an absorption wavelength below 370 nm. In the presence of FA, as the formaldehyde concentration increases, the absorbance peak increases and appears at 414 nm (Figure 30b). For 1,3-diphenyl-1,3-propanedione, in the absence of FA, the conjugated electrons of 1,3-diphenyl-1,3-propanedione show an absorption wavelength below 400 nm. In the presence of FA, as the formaldehyde concentration increases, the absorbance peak increases, and a peak appears at 424 nm (Figure 30c). An absorbance change at 407, 414, and 424 nm as a function of FA concentration is recorded. The absorbance peak of acetylacetone at 407 nm shows a direct relationship with formaldehyde concentration up to the value of 250 ppb. The absorbance peak of 1-phenyl-1,3-butanedione shows saturation

after formaldehyde concentration increases beyond 140 ppb. The absorbance peak of 1,3-diphenyl-1,3-propanedione shows a decrease as formaldehyde concentration increases beyond 140 ppb.⁴⁹

Acetoacetanilide reacts with FA in the presence of ammonia through a cyclization process for FA detection (Figure 31).⁵⁰

In the presence of ammonium acetate and acetic acid, methyl acetoacetate reacts with FA for FA detection (Figure 32).⁵¹

Three different concentrations of formaldehyde are used with 300 μL of methyl acetoacetate, and the reaction rates were studied. It is found that reaction of methyl acetoacetate with formaldehyde takes 6 h to complete. The reaction time taken by acetyl acetate is found to be 4 h, which is faster than methyl acetoacetate. The absorption peaks for acetyl acetone are found to be 410 nm, and that of methyl acetoacetate is found to be 376 nm. The same observation is noted with color change. A weaker yellow color change is observed with methyl acetoacetate than with acetylacetone because of the presence of ester groups.⁵¹

Acetylacetone showed better absorbance changes than the other two sensor elements. For acetylacetone, a porous glass surface is the site for both the reactions of formation and decomposition, while in case of the 1-phenyl-1,3-butanedione, only the formation reaction occurs on the porous glass surface. The reaction speed was also higher at 20 $^{\circ}\text{C}$ for acetylacetone. Acetylacetone is found to be better for short-term detection, while 1-phenyl-1,3-butanedione is better for long-term detection. The Hantzsch reaction is a slow reaction and is temperature dependent. Temperature control is an important parameter for Hantzsch reaction.⁵²

As the formaldehyde concentration increases, the absorbance peak increases, and the fluorescence intensity of the compound is increased. A maximum absorption wavelength of 368 nm is obtained with acetoacetanilide in the presence of FA. An increase in the blank reagent absorption can also result in increasing concentration of acetoacetanilide. However, the flow injection method employed showed a detection limit of 3×10^{-9} M and was found to be superior in terms of sensitivity compared with other methods. The reactions are however highly pH dependent.⁵³

4.4. Furazan. Ge et al. synthesized an FAP probe through an aldimine condensation reaction between 7-nitrobenzo-2-oxa-1,3-diazolyl chloride (NBD), dichloromethane, hydrazine, and methanol (Figure 33).^{52–54} The reaction mechanism of the FAP probe with the FA was based on a nucleophilic reaction. When the probe was present in the Free State, the PET mechanism was operative, where the hydrazine group acted as an electron donor and transferred electrons to NBD. In this case, the PET acted as an OFF mechanism, whereas hydrazine acted as a fluorescence quencher. After FA addition, a Schiff base formed ($\text{C}=\text{N}$), which blocked the transfer of electrons. Consequently, FA acted as a turn-on species for NBD that aided in the detection of FA (Figure 34).⁵⁴

The concentration of the FAP probe played a determining role in the detection of FA. With the increase in the concentration of the probe, the sensitivity increases. The concentration of FA increases from 0 mg L^{-1} to 0.8 mg L^{-1} . As a result, the fluorescence intensity increases, and the maximum peak appears at 550 nm. The detection limit of the proposed study reached 0.89 $\mu\text{g L}^{-1}$, and the fluorescence enhancement of up to 30 times was observed (Figure 35).⁵⁴

4.5. BODIPY-Substituted Hydrazine. Chen et al. showed that the BHA probe itself is weakly fluorescent because of the presence of the strong donor group $\text{NH}-\text{NH}_2$. This strong donor group contributes to the twisted internal charge transfer (TICT) process when it is excited. The TICT process has a very low fluorescence efficiency and resembles the PET process. However, upon FA addition, an $\text{NH}-\text{N}=\text{NH}_2$ moiety is formed, which is a weak donor group. When this functional group is excited, it undergoes the ICT process, and a prominent turn-on process is obtained (Figure 36).⁵⁵

The BHA probe has the advantages of low cytotoxicity and high sensitivity with a detection limit of 0.18 μM , and if a fast response time is less than 30 min, it can be used endogenously for the detection of FA in HeLa cells. The use of this probe for other types of living cells has not been identified.⁵⁶ However, using another BODIPY-based probe containing two moieties, one being BODIPY and the second an amine, BOD- NH_2 has been synthesized.⁵⁶ This newly synthesized probe has advantages over the previous one as it is reversible in nature and can be used for a wide variety of living cells. It can be applied directly to the cytoplasm. It can be used for FA detection in dissected organs and fresh hippocampus of mice. Guo and co-workers reported BODIPY-OPDA for detecting formaldehyde with a very low detection limit (0.104 μM).⁵⁷

4.6. Pillar[5]arene. DP5J, an ultrasensitive probe based on pillar[5]arene derivatives, was formed for FA detection in both gas and solution.⁵⁸ The probe was synthesized by incorporating thioacetylhydrazine groups on the pillar[5]arene moiety, as shown in Figure 37.

The hydride group served as a reactive site for FA sensing. A catalyst ($(\text{CF}_3\text{SO}_3)_2\text{Bi}$) was added to improve the FA sensitivity of DP5J. As a result, the detection time was reduced from 30 to 7.5 s. The FA detection limit of DP5J was 3.27×10^{-9} M (Figure 38).⁵⁸

Upon FA addition, DP5J reacted with FA to form a carbinolamine intermediate (DP5J-OH) through hydroxymethylation. DP5J-OH further underwent dehydration to give an imine product DP5J-S. DP5J-OH and DP5J-S self-assembled through $\pi-\pi$ interactions between pillar[5]arene groups and intermolecular hydrogen bond formation. Because of this self-assembly, aggregates were formed, which restricted intramolecular motion. This induced AIE and a strong fluorescence emission wavelength at 450 nm were obtained.

Pillar[5]arene was advantageously ultrasensitive to FA, with a detection limit of 3.27 nM. It has a very fast response time of 7.5 s, but the $(\text{CF}_3\text{SO}_3)_2\text{Bi}$ catalyst is needed for this fast detection.⁴¹ Recently, a pillar[5]arene-based fluorescent supramolecular polymer with vaporochromic behavior was used for the detection of FA.⁵⁹

5. CONCLUSION

There have been several ways put forth so far for FA detection. However, there are significant issues with these methods; for instance, some are expensive and can react with other aldehydes easily; others form carbonates when a strong base is present; others have slow color development and sensitivity; and some call for instantaneous measurements of sample solutions because the intermediate is unstable. FA sensing techniques have allowed for more precise detection and real-time measurement by transferring FA into an aqueous solution using flow injection analysis, as in the Hantzsch reaction. Such a strategy should use more targeted sensors.

The requirement of stoichiometric amounts of fluorescent probes to generate a signal is a significant barrier to the above devised strategies, leading to ineffective and time-consuming processes. Additionally, these also disrupt native analyte homeostasis and local concentration levels. Therefore, developing reversible fluorescent probes for the recycling of these substances is crucially necessary to stop the production of chemical sludges. This thorough comprehension of the mechanisms of fluorescent probes could help chemists create reversible probes that can help reduce the restrictions among the available chemical instruments and can be used for selective FA detection.

AUTHOR INFORMATION

Corresponding Authors

Moaz M. Abdou – Egyptian Petroleum Research Institute, Nasr City 11727 Cairo, Egypt; orcid.org/0000-0003-0253-5714; Email: moaz.chem@gmail.com

Imtiaz Ahmad – Department of Chemistry, Fatima Jinnah Women University, 46000 Rawalpindi, Pakistan; orcid.org/0000-0003-1599-6181; Email: imtiaz.ahmad14@outlook.com

Tahir Muhmood – College of Science, Nanjing Forestry University, Nanjing 210037, China; orcid.org/0000-0002-7441-1617; Email: muhmoodtahir@yahoo.com

Authors

Ahmed Abu-Rayyan – Faculty of Arts & Science, Applied Science Private University, Amman 11931, Jordan

Nawal H. Bahtiti – Faculty of Arts & Science, Applied Science Private University, Amman 11931, Jordan

Samir Bondock – Chemistry Department, Faculty of Science, King Khalid University, 9004 Abha, Kingdom of Saudi Arabia; Chemistry Department, Faculty of Science, Mansoura University, 35516 Mansoura, Egypt; orcid.org/0000-0003-1622-1599

Mohammed Abohashrh – Department of Basic Medical Sciences, College of Applied Medical Sciences, King Khalid University, Abha 61421, Kingdom of Saudi Arabia

Habiba Faheem – Department of Chemistry, Fatima Jinnah Women University, 46000 Rawalpindi, Pakistan

Nimra Tehreem – Department of Chemistry, Fatima Jinnah Women University, 46000 Rawalpindi, Pakistan

Aliya Yasmeeen – Department of Chemistry, Fatima Jinnah Women University, 46000 Rawalpindi, Pakistan

Shiza Waseem – Department of Chemistry, Fatima Jinnah Women University, 46000 Rawalpindi, Pakistan

Tayabba Arif – Department of Chemistry, Fatima Jinnah Women University, 46000 Rawalpindi, Pakistan

Amal H. Al-Bagawi – Department of Chemistry, College of Science, University of Ha'il, Ha'il City, Hail 2440, Kingdom of Saudi Arabia

Complete contact information is available at: <https://pubs.acs.org/10.1021/acsomega.2c07724>

Notes

The authors declare no competing financial interest.

ACKNOWLEDGMENTS

The authors extend their appreciation to the Deanship of Scientific Research at King Khalid University for funding this work through research group projects (Grant nos. RGP.1/98/43 and RGP.1/368/43). This work is dedicated to the memory

of the pure soul of Professor Mohamed Abbas El-Metwally (D.Sc.), who was working at the Department of Chemistry, Faculty of Science, Mansoura University, Egypt.

ABBREVIATIONS

AIE	Aggregation-induced emission
BHA	BODIPY-substituted hydrazine
BODIPY	Boron-dipyrromethene
CIE	Commission Internationale de l'Éclairage 3
DMSO	Dimethyl sulfoxide
ESI	Electrospray ionization
FA	Formaldehyde
FAP-I	Formaldehyde probe-1
HBT-FA	2-(2-Hydroxyphenyl)benzothiazole formaldehyde probe
HCy	Heptamethine cyanine
HOMO	Highest occupied molecular orbital
ICT	Intramolecular charge transfer
LED	Light-emitting diode
LOD	Limit of detection
LUMO	Lowest unoccupied molecular orbital
MCF-7	Michigan cancer foundation-7
NBD	7-Nitrobenzo-2-oxa-1,3-diazolyl
PET	Photoinduced electron transfer
TICT	Twisted intramolecular charge transfer
TPE	Tetraphenylethene

REFERENCES

- (1) Yuan, Z.; Yang, C.; Meng, F. Strategies for Improving the Sensing Performance of Semiconductor Gas Sensors for High-Performance Formaldehyde Detection: A Review. *Chemosensors* **2021**, *9* (7), 179.
- (2) WHO. *WHO Guidelines for Indoor Air Quality: Selected Pollutants*; WHO, 2010; p 484.
- (3) ATSDR. *ATSDR's substance priority list*. Agency for Toxic Substances and Disease Registry; 2019. Accessed November 24, 2020, from <https://www.atsdr.cdc.gov/spl/index.html>.
- (4) Wan, Y.; Fan, X.; Zhu, T. Removal of low-concentration formaldehyde in air by DC corona discharge plasma. *Chem. Eng. J.* **2011**, *171* (1), 314–319.
- (5) WHO. *WHO Guidelines for Indoor Air Quality: Selected Pollutants*; WHO, 2010; p 484.
- (6) Chung, P.; Tzeng, C.; Ke, M.; Lee, C. Formaldehyde gas sensors: A Review. *Sensors* **2013**, *13* (4), 4468–4484.
- (7) Kukkar, D.; Vellingiri, K.; Kaur, R.; Bhardwaj, S.; Deep, A.; Kim, K. Nanomaterials for sensing of formaldehyde in air: Principles, applications, and performance evaluation. *Nano Res.* **2019**, *12* (2), 225–246.
- (8) Xu, Z.; Chen, J.; Hu, L.; Tan, Y.; Liu, S.; Yin, J. Recent advances in formaldehyde-responsive fluorescent probes. *Chin. Chem. Lett.* **2017**, *28* (10), 1935–1942.
- (9) Liao, C.; Shi, J.; Zhang, M.; Dalapati, R.; Tian, Q.; Chen, S.; Wang, C.; Zang, L. Optical chemosensors for the gas phase detection of aldehydes: mechanism, material design, and application. *Mater. Adv.* **2021**, *2* (19), 6213–6245.
- (10) Pan, S.; Roy, S.; Choudhury, N.; Behera, P.; Sivaprakasam, K.; Ramakrishnan, L.; De, P. From small molecules to polymeric probes: recent advancements of formaldehyde sensors. *Sci. Technol. Adv. Mater.* **2022**, *23* (1), 49–63.
- (11) Lin, Q.; Fan, Y. Q.; Gong, G. F.; Mao, P. P.; Wang, J.; Guan, X. W.; Liu, J.; Zhang, Y. M.; Yao, H.; Wei, T. B. Ultrasensitive Detection of Formaldehyde in Gas and Solutions by a Catalyst Preplaced Sensor Based on a Pillar[5]arene Derivative. *ACS Sustainable Chem. Eng.* **2018**, *6* (7), 8775–8781.
- (12) Bi, A.; Gao, T.; Cao, X.; Dong, J.; Liu, M.; Ding, N.; Liao, W.; Zeng, W. A novel naphthalimide-based probe for ultrafast, highly

- selective and sensitive detection of formaldehyde. *Sens. Actuators, B* **2018**, *255*, 3292–3297.
- (13) El-Mahalawy, A. M.; Abdou, M. M.; Wassel, A. R. Physical and optoelectronic characteristics of novel low-cost synthesized coumarin dye-based metal-free thin films for light sensing applications. *Mater. Sci. Semicond. Process.* **2022**, *137*, 106225.
- (14) Abdou, M. M. Synopsis of recent synthetic methods and biological applications of phosphinic acid derivatives. *Tetrahedron* **2020**, *76* (25), 131251.
- (15) Abdou, M. M.; El-Saeed, R. A. Innovative and potential chemical transformation of phosphinic acid derivatives and their applications in the synthesis of drugs. *Bioorg. Chem.* **2019**, *90*, 103039.
- (16) Abdou, M. M.; Seferoglu, Z.; Fathy, M.; Akitsu, T.; Koketsu, M.; Kellow, R.; Amigues, E. Synthesis and chemical transformations of 3-acetyl-4-hydroxyquinolin-2(1H)-one and its N-substituted derivatives: Bird's eye view. *Res. Chem. Intermed.* **2019**, *45* (3), 919–934.
- (17) Abdou, M. M.; El-Saeed, R. A.; Elattar, K. M.; Seferoglu, Z.; Boukouvalas, J. Advancements in tetrionic acid chemistry. Part 2: Use as a simple precursor to privileged heterocyclic motifs. *Mol. Divers.* **2016**, *20* (4), 989–999.
- (18) Misra, R.; Bhattacharyya, S. P. *Intramolecular Charge Transfer: Theory and Applications*, 1st ed.; Wiley-VCH Verlag GmbH Co. KGaA.; 2018; pp 16–17.
- (19) Natali, M.; Campagna, S.; Scandola, F. Photoinduced electron transfer across molecular bridges: electron- and hole-transfer superexchange pathways. *Chem. Soc. Rev.* **2014**, *43* (12), 4005–4018.
- (20) Ma, Y.; Chen, Q.; Pan, X.; Zhang, J. Insight into Fluorescence Imaging and Bioorthogonal Reactions in Biological Analysis. *Top. Curr. Chem.* **2021**, *379* (2), 1–21.
- (21) Zhao, Z.; Zhang, H.; Lam, J.; Tang, B. Aggregation-Induced Emission: New Vistas at the Aggregate Level. *Angew. Chem., Int. Ed.* **2020**, *59* (25), 9888–9907.
- (22) Allouch, A.; Guglielmino, M.; Bernhardt, P.; Serra, C.; Le Calvé, S. Transportable, fast and high sensitive near real-time analyzers: formaldehyde detection. *Sens. Actuators, B* **2013**, *181*, 551–558.
- (23) Li, Q.; Sritharathikhun, P.; Oshima, M.; Motomizu, S. Development of novel detection reagent for simple and sensitive determination of trace amounts of formaldehyde and its application to flow injection spectrophotometric analysis. *Anal. Chim. Acta* **2008**, *612* (2), 165–172.
- (24) Manna, S.; Achar, T.; Mondal, S. Recent advances in selective formaldehyde detection in biological and environmental samples by fluorometric and colorimetric chemodosimeters. *Anal. Methods* **2021**, *13* (9), 1084–1105.
- (25) Tantipanaporn, A.; Ka-Yan Kung, K.; Sit, H.-Y.; Wong, M.-K. Quinolinium-based fluorescent probes for formaldehyde detection in aqueous solution, serum, and test strip via 2-aza-Cope rearrangement. *RSC Adv.* **2022**, *12* (18), 11543–11547.
- (26) Lee, H.; Kim, K.; Kim, M.; Kim, C. Recent Advances in Catalytic [3,3]-Sigmatropic Rearrangements. *Catalysts* **2022**, *12* (2), 227.
- (27) Gao, T.; Cao, X.; Bi, A.; Dong, J.; Huang, S.; Huang, X.; Wen, S.; Zeng, W. An Aza-Cope mediated fluorescent probe based on aggregation-induced emission for highly selective and sensitive detection of formaldehyde in living cells and tissues. *Sens. Actuators, B* **2018**, *273*, 1139–1145.
- (28) Xu, J.; Zhang, Y.; Zeng, L.; Liu, J.; Kinsella, J.; Sheng, R. A simple naphthalene-based fluorescent probe for high selective detection of formaldehyde in toffees and HeLa cells via aza-Cope reaction. *Talanta* **2016**, *160*, 645–652.
- (29) Liu, J.; Li, K.; Xue, P.; Xu, J. Cell-permeable fluorescent indicator for imaging formaldehyde activity in living systems. *Anal. Biochem.* **2022**, *652*, 114749.
- (30) Pan, S.; Roy, S.; Choudhury, N.; Behera, P.; Sivaprakasam, K.; Ramakrishnan, L.; De, P. From small molecules to polymeric probes: recent advancements of formaldehyde sensors. *Sci. Technol. Adv. Mater.* **2022**, *23* (1), 49–63.
- (31) Brewer, T.; Chang, C. An Aza-Cope reactivity-based fluorescent probe for imaging formaldehyde in living cells. *J. Am. Chem. Soc.* **2015**, *137* (34), 10886–10889.
- (32) Ohata, J.; Bruemmer, K.; Chang, C. Activity-based sensing methods for monitoring the reactive carbon species carbon monoxide and formaldehyde in living systems. *Acc. Chem. Res.* **2019**, *52* (10), 2841–2848.
- (33) Zhou, Y.; Yan, J.; Zhang, N.; Li, D.; Xiao, S.; Zheng, K. A ratiometric fluorescent probe for formaldehyde in aqueous solution, serum and air using aza-cope reaction. *Sens. Actuators, B* **2018**, *258*, 156–162.
- (34) Wu, Y.; Zheng, Z.; Wen, J.; Li, H.; Sun, S.; Xu, Y. Imaging of formaldehyde in live cells and plants utilizing small molecular probes with large Stokes shifts. *Sens. Actuators, B* **2018**, *260*, 937–944.
- (35) Yang, H.; Fang, G.; Guo, M.; Ning, P.; Feng, Y.; Yu, H.; Meng, X. A ratiometric two-photon fluorescent probe for selective detection of endogenous formaldehyde via Aza-Cope reaction. *Sens. Actuators, B* **2018**, *270*, 318–326.
- (36) Ning, P.; Dong, P.; Geng, Q.; Bai, L.; Ding, Y.; Tian, X.; Shao, R.; Li, L.; Meng, X. A two-photon fluorescent probe for viscosity imaging in vivo. *J. Mater. Chem. B* **2017**, *5* (15), 2743–2749.
- (37) Quan, T.; Liang, Z.; Pang, H.; Zeng, G.; Chen, T. A ratiometric ESIPT probe based on 2-aza-Cope rearrangement for rapid and selective detection of formaldehyde in living cells. *Analyst* **2022**, *147* (2), 252–261.
- (38) Sani, U.; Na'ibi, H.; Dailami, S. In vitro antimicrobial and antioxidant studies on N-(2-hydroxybenzylidene) pyridine-2-amine and its M(II) complexes. *NJBAS* **2018**, *25* (1), 81.
- (39) Wechakorn, K.; Supalang, S.; Suanpai, S. A Schiff base-based ratiometric chemosensor conjugated NBD derivative with the large Stokes shift for formaldehyde detection. *Tetrahedron* **2020**, *76* (34), 131411.
- (40) Hidayah, N.; Purwono, B.; Pranowo, H. D. Symmetrical azine colorimetric and fluorometric turn-off chemosensor for formaldehyde detection. *JSM* **2019**, *48* (10), 2161–2167.
- (41) Wei, K.; Ma, L.; Ma, G.; Ji, C.; Yin, M. A two-step responsive colorimetric probe for fast detection of formaldehyde in weakly acidic environment. *Dyes Pigm.* **2019**, *165*, 294–300.
- (42) Lu, X.; Li, R.; Han, B.; Hou, X.; Kang, Y.; Zhang, Y.; Wang, J. J. Fluorescence sensing of formaldehyde and acetaldehyde based on responsive inverse opal photonic crystals: A Multiple-application detection platform. *ACS Appl. Mater. Interfaces* **2021**, *13* (11), 13792–13801.
- (43) Ding, N.; Li, Z.; Hao, Y.; Yang, X. A new amine moiety-based near-infrared fluorescence probe for detection of formaldehyde in real food samples and mice. *Food Chem.* **2022**, *384*, 132426.
- (44) Zhou, W.; Dong, H.; Yan, H.; Shi, C.; Yu, M.; Wei, L.; Li, Z. HCHO-reactive molecule with dual-emission-enhancement property for quantitatively detecting HCHO in near 100% water solution. *Sens. Actuators, B* **2015**, *209*, 664–669.
- (45) Kukhta, N.; Bryce, M. Dual emission in purely organic materials for optoelectronic applications. *Mater. Horiz.* **2021**, *8* (1), 33–55.
- (46) Ji, H.; Duan, W.; Huo, Y.; Liu, W.; Huang, X.; Wang, Y.; Gong, S. Highly sensitive fluorescence response of [2.2]paracyclophane modified D-A type chromophores to trace water, pH, acidic gases and formaldehyde. *Dyes Pigm.* **2022**, *205*, 110491.
- (47) Chen, W.; Han, J.; Wang, X.; Liu, X.; Liu, F.; Wang, F.; Yu, R. Q.; Jiang, J. H. Aggregation-induced emission-based fluorescence probe for fast and sensitive imaging of formaldehyde in living cells. *ACS Omega* **2018**, *3* (10), 14417–14422.
- (48) Zhao, X.; Ji, C.; Ma, L.; Wu, Z.; Cheng, W.; Yin, M. An aggregation-induced emission-based “turn-on” fluorescent probe for facile detection of gaseous formaldehyde. *ACS Sens.* **2018**, *3* (10), 2112–2117.
- (49) Maruo, Y.; Nakamura, J.; Uchiyama, M. Development of formaldehyde sensing element using porous glass impregnated with β -diketone. *Talanta* **2008**, *74* (5), 1141–1147.
- (50) LI, Q.; Sritharathikhun, P.; Motomizu, S. Development of novel reagent for hantzsch reaction for the determination of formaldehyde

by spectrophotometry and fluorometry. *Anal. Sci.* **2007**, *23* (4), 413–417.

(51) Bunkoed, O.; Davis, F.; Kanatharana, P.; Thavarungkul, P.; Higsion, S. Sol-gel based sensor for selective formaldehyde determination. *Anal. Chim. Acta* **2010**, *659* (1–2), 251–257.

(52) Kochetkova, M.; Timofeeva, I.; Bulatov, A. A derivatization and microextraction procedure with organic phase solidification on a paper template: Spectrofluorometric determination of formaldehyde in milk. *Spectrochim. Acta, Part A* **2021**, *263*, 120160.

(53) Li, Q.; Oshima, M.; Motomizu, S. Flow-injection spectrofluorometric determination of trace amounts of formaldehyde in water after derivatization with acetoacetanilide. *Talanta* **2007**, *72* (5), 1675–1680.

(54) Ge, H.; Liu, G.; Yin, R.; Sun, Z.; Chen, H.; Yu, L.; Su, P.; Sun, M.; Alamry, K. A.; Marwani, H. M.; Wang, S. An aldimine condensation reaction based fluorescence enhancement probe for detection of gaseous formaldehyde. *Microchem. J.* **2020**, *156*, 104793.

(55) Chen, H.; Li, H.; Song, Q. BODIPY-Substituted Hydrazine as a Fluorescent Probe for Rapid and Sensitive Detection of Formaldehyde in Aqueous Solutions and in Live Cells. *ACS Omega* **2018**, *3* (12), 18189–18195.

(56) Song, X.; Han, X.; Yu, F.; Zhang, J.; Chen, L.; Lv, C. A reversible fluorescent probe based on C–N isomerization for the selective detection of formaldehyde in living cells and in vivo. *Analyst* **2018**, *143* (2), 429–439.

(57) Cao, T.; Gong, D.; Han, S. C.; Iqbal, A.; Qian, J.; Liu, W.; Qin, W.; Guo, H. BODIPY-based fluorescent sensor for imaging of endogenous formaldehyde in living cells. *Talanta* **2018**, *189*, 274–280.

(58) Lin, Q.; Fan, Y. Q.; Gong, G. F.; Mao, P. P.; Wang, J.; Guan, X. W.; Liu, J.; Zhang, Y. M.; Yao, H.; Wei, T. B. Ultrasensitive detection of formaldehyde in gas and solutions by a catalyst preplaced sensor based on a Pillar[5]arene derivative. *ACS Sustainable Chem. Eng.* **2018**, *6* (7), 8775–8781.

(59) Shi, B.; Chai, Y.; Qin, P.; Zhao, X. X.; Li, W.; Zhang, Y. M.; Wei, T. B.; Lin, Q.; Yao, H.; Qu, W. J. Detection of aliphatic aldehydes by a Pillar[5]arene-based fluorescent supramolecular polymer with vaporchromic behavior. *Chem.: Asian J.* **2022**, *17* (5), No. e202101421.